Supplemental Experimental Procedures

Cardiomyocyte cell sheet transplantation. Following coronary artery ischemia reperfusion, the animals were observed for 30 minutes. Day-10 beating human induced pluripotent stem cells derived cardiomyocytes (hiPSC-CM) cell sheet containing 10 $x10^6$ cells was first suspended in 25 mg/ml fibronogen, then was placed over area of myocardial infarction. To enhance the fibrin CMs-sheet attachment, the epicardial surface of the anterior wall was lightly punctured to induce the endogenous thrombin to enhance the attachment of hiPSC-CM cell sheet. This surface preparation also promotes interaction between the hiPSC-CM sheet and recipient myocardium. In addition, 80 u/ml of thrombin was also applied to the surface of the injured area. The chest will be closed by layers, the pneumothorax evacuated, and the animals allowed to recover.

hiPSCs were differentiated into CMs via the Sandwich method (Zhang et al., 2012). Clusters of contracting cells were collected 14 or 15 days after initiating differentiation, washed in Hanks Balanced Salt Solution (HBSS, Life Technologies, USA), and incubated in HBSS containing 100 U/mL collagenase IV for 10 minutes at 37 ºC with gentle shaking; then, 0.25% trypsin/EDTA was added, and the enzyme solution was neutralized with fetal bovine serum 5 minutes later. The cells were resuspended in RPMI/B27 medium and cultured on cell culture dishes for at least three hours; then, the non-attached cells (or clusters of cells) were collected and cultured on Matrigel-coated cell culture dishes.

To characterize the hiPSC-CMs, cells were fixed with 4% paraformaldehyde for 20 minutes at room temperature, permeabilized in 0.1% Triton X-100 at 4 ºC for 10 min, and then blocked with UltraV block (Thermo Scientific, USA) for 7 min. Primary antibodies (mouse anti-SMHC, [Santa Cruz Biotech., USA], mouse anti-α-sarcomeric actin [Sigma-Aldrich, USA], mouse anti-cTnT [Thermo Scientific, USA], rabbit anti-cTnI [Abcam, USA], rabbit anti-MLC2v [Proteintech Group, USA]), were added into the UltraV block buffer, and the cells were incubated overnight at 4 ºC; then, secondary antibodies conjugated with fluorescent markers (Jackson ImmunoResearch Lab. West Grove, PA, USA) were added. The cells were incubated for 1 hour at room temperature and then stained with DAPI, washed, and examined under a fluorescence microscope (Olympus, Japan).

In-vitro cytoprotection assays hiPSC-CMs ($4x10^4$) were seeded into 12-well plates that had been precoated with Matrigel and then cultured overnight at 37 ºC in RPMI1640+B27. After washing with DPBS, 0.3 mL of fresh or conditioned MEM medium was added to each well; the conditioned medium consisted of a 1:1 mixture of medium collected from hiPSC-ECs and hiPSC-SMCs that had been cultured in serum- and glucose-free MEM medium for 48 hours. The hiPSC-CMs were cultured under hypoxic conditions (5% CO_2, 94% N_2, and 1% O_2) for 48 hours; then, the supernatant was collected for assessments of cytotoxicity and apoptosis.

Cytotoxicity was determined by measuring the intensity of lactate dehydrogenase (LDH) fluorescence in the supernatant via the CytoTox-One Homogenous Membrane Integrity assay (Promega, USA) as directed by the manufacturer's instructions. The excitation and emission wavelengths were 560 nm and 590 nm, respectively, and the experiment

was repeated at least three times with duplicate samples in each experiment. Measurements for cells cultured in the conditioned medium were normalized to measurements for cells in the unconditioned medium and expressed as percentage.

Apoptosis was evaluated with an In-situ Cell Death Detection Kit (Roche Applied Science, Germany) as directed by the manufacturer's instructions; 3-4 wells were analyzed per condition, and 4-6 high-power images were taken for each well. Both the total number of cells and the number of TUNEL+ cells were determined, and apoptosis was quantified as the ratio of the number of TUNEL+ nuclei to the total number of nuclei per high-power field.

Synthesis of IGF-containing microspheres and patch manufacture Olive oil was heated to 45 ºC and 5 mL of 10% gelatin (type B, Sigma-Aldrich, USA) solution was heated to 50 ºC in a water bath; then, the gelatin was added to the olive oil, stirred, and cooled to 5 ºC. Twenty-five minutes later, chilled (4 ^{o}C) acetone was added to the olive oil for 1 hour to induce microsphere formation; then, the microspheres were collected, washed 5 times to remove the olive oil, air-dried at 4 ^{o}C, and resuspended in 70% ethanol supplemented with 0.25% glutaraldehyde overnight to induce cross-linking. The mixture was neutralized with 100 mM glycine, washed 5 times with 70~100% ethanol, and then freeze dried (Figure S2).

To determine the rate at which IGF was released from the microspheres, a fibrin patch was created by loading 5 mg of IGF-containing microspheres with 5 µg IGF-1 (R&D Systems, USA) and then combining the microspheres with 1 mL fibrinogen solution (25 mg/mL) and 1 mL thrombin (80 NIH units/mL, Sigma Aldrich, USA) supplemented with 2 µL 400 mM $CaCl_2$ and 200 mM Ɛ-aminocaproic acid (Sigma Aldrich, USA). The patch was cultured with 2 mL MEM medium in a 6-well plate, and 1 mL of the conditioned medium was collected and replaced with 1 mL of fresh MEM medium each day. The IGF-1 concentration in the conditioned MEM medium was determined with a Human IGF-I Quantikine ELISA Kit (R&D Systems, USA), as directed by the manufacturer's instructions.

Porcine IR injury model and treatment The induction of experimental myocardial IR injury has been described previously (Xiong et al., 2011b; Zeng et al., 2007). Briefly, the D1 branch of the left anterior descending and the M1 branch of the left circumflex coronary arteries were ligated with 4.0 polypropylene sutures. Occlusion was maintained for 60 minutes; then, the myocardium was reperfused for 15 min, the experimental treatment was administered, the chest was closed in layers, and the animals were allowed recover. Because the transplanted cells were derived from human cells, animals in all experimental groups received cyclosporine (15 mg/kg per day with food) for immunosuppression from 3 days before injury until sacrifice.

Cardiac MRI MRI assessments of cardiac function were performed with a 1.5-Tesla clinical scanner (Siemens Aera, Siemens Medical Systems, Islen NJ), a phased-array 4-channel surface coil, and ECG gating as described previously (Feygin et al., 2007; Jerosch-Herold et al., 2002; Xiong et al., 2011a; Xiong et al., 2012). Briefly, the MRI protocol consisted of: 1) localizing scouts to identify the long- and short-axis of the heart, 2) short- and long-axis cine for the measurement of global cardiac function and 3) delayed contrast-enhancement (DE) MRI for the assessment of scar size. Steady-state

free precession “True-FISP” cine imaging was performed with the following MR parameters: TR = 3.1 ms, TE = 1.6 ms, flip angle = 65^{o}, matrix size = 256 x 192, field of view = 300 mm x 225 mm, slice thickness = 6 mm (4 mm gap between slices); 25 phases were acquired across the cardiac cycle. Perfusion images were acquired with a cardiac-gated, T1-weighted turbo-FLASH sequence with a saturation-recovery magnetization preparation (TR = 2.4 ms, TE = 1.2 ms, TI = 120 ms, flip angle = 12^{o}, matrix size = 192 x 103, field of view = 300 mm x 225 mm, slice thickness = 8 mm). The contrast agent (0.04 mmol/kg Gd-DTPA; Magnevist, Berlex, Wayne, NJ) was administered as a bolus intravenous injection at a rate of 7 mL/s. DE MR images were acquired by using an ECG-gated turbo-FLASH sequence along the short axis of the LV from base to apex; sequence parameters were: TR = 16 ms, TE = 4 ms, TI = 270-320 ms, flip angle = 25^{o}, matrix size = 256 x 208, field of view = 300 mm x 243 mm, slice thickness = 6 mm (0 mm gap between slices) and two signal averages. The inversion time (TI) was chosen to nullify signal intensity from normal myocardium. Global function and regional wall thickness data were computed from the short-axis cine images; CIMRA (CSON Medical, Minneapolis, MN) was used for manual segmentation of the endocardial and epicardial surfaces (from base to apex) at both end-diastole and end-systole. Infarct size was calculated from the DE-MR images and presented as the ratio of scar surface area to the total LV surface area; CIMRA was used to semi-automatically segment regions of non-viable tissue.

hiPSC-EC, -SMC, and -CM engraftment rate Engraftment was evaluated via quantitative, real-time PCR (qRT-PCR) assessments of the human Y-chromosome from 3 (CM and CM+EC+SMC groups) or 4 (Cell+Patch group) animals in each experimental group. The LV free wall was cut into 6 short-axis rings (R1-6), and each ring was sequentially cut into 8 or 9 samples (S1-S9) (Zeng et al., 2007). S2-S5 of R3-R5 (i.e, from the site of cell and/or patch administration) were collected, digested overnight at 56^{o}C with proteinase K, and then the total DNA was isolated from the digested buffer with a QIAGEN DNA isolation kit. The number of cells in each sample was determined by comparing the number of cycles required for each sample to a standard curve calculated from the DNA of known quantities of undifferentiated hiPSCs; then, the total number of cells in each heart was calculated as the sum of all samples from the same animal, and the engraftment rate was calculated as the number of cells in each animal divided by the number of cells administered ($6x10^{6}$). Analyses were performed with the SYBR Green kit (Fermentas, USA) on an Eppendorf Realplex PCR system (Eppendorf, USA) as previously described (Ye et al., 2007) with the following primers: sense, ATCAGCCTAGCCTGTCTTCAGCAA;
anti-sense, TTCACGACCAACAGCACAGCAATG.”

Histochemical and immunohistochemical evaluations The LV free wall was cut vertically into 6 rings (R1-R6), and each ring was sequentially cut into 8 or 9 samples (S1-S9). S3 and S4 of R3 and R4 (i.e, from the site of cell and/or patch administration) were collected and embedded for cryosectioning or paraffin-sectioning.

The transplanted patches were identified by staining paraffin-embedded sections with an Accustain (Masson) Trichrome Stains kit (Sigma-Aldrich, USA). Cell lineages were determined in 7-μm cryosections or 5-μm paraffin-embedded sections via fluorescence immunostaining for the expression of GFP (goat anti-GFP; Abcam, USA), CD31 (rabbit anti-CD31, Santa Cruz, USA), SMA (mouse anti-SMA, Sigma-Aldrich, USA), and cTnT

(mouse anti-cTnT, Thermo Scientific, USA**;** R&D systems, USA); primary antibodies were visualized with fluorescent secondary antibodies (Jackson ImmunoResearch Lab, USA). hiPSC-ECs were identified with antibodies specific for the human isoform of CD31 (hCD31, BD Pharmingen, USA). Engrafted hiPSC-ECs were identified by hCD31 expression, engrafted hiPSC-SMCs were identified by the expression of both GFP and SMA, and engrafted hiPSC-CMs were identified by the expression of both GFP and cTnT. The inflammatory response to injury and treatment was evaluated by immunofluorescent staining with anti-CD11b antibodies (Abcam, USA). Vascular density was evaluated by counting the number of vascular structures that were positive for either CD31 or SMA expression; then, the images used for the CD31 and SMA evaluations were superimposed, and arteriole density was evaluated by counting the number of structures that expressed both CD31 and SMA. Cells and vessels were counted in 6-8 HPFs per section, 8-10 sections per animal.

In vivo cardiac ^{31}P MR spectroscopic assessments In vivo measurements of myocardial PCr/ATP ratios and ATP turnover rate were obtained via an open-chest ^{31}P MRS-MST protocol as described previously (Xiong et al., 2011a; Xiong et al., 2012; Xiong et al., 2013). Measurements were performed on a 65 cm-bore 9.4-T magnet interfaced with a Vnmrj console (Varian, CA). Radiofrequency transmission and MRS signal detection were performed with a double-tuned (^{1}H and ^{31}P) surface coil (28-mm diameter) sutured directly to the LV epicardium over the peri-infarct region. Measurements were obtained under baseline conditions and after a high cardiac workstate was induced via catecholamine injection (20 µg/kg per minute dobutamine and 20 µg/kg per minute dopamine, administered via intravenous injection).

Materials and methods for proteomics

Tissue sample preparation for mass spectrometry analyses A total of 3 groups were studied, including normal (NL), myocardial infarction (MI), and MI treated iPSC-vascular cells (MI+iPSC-VC). Each group has 5 biological replicates. Approximately, 50 mg of each swine heart tissue sample was used for following protein extraction. All of the processes of tissue extraction were performed in a cold room (4 °C). The frozen pig heart tissue samples were cut into small pieces (approximate 2 mm^3) and immediately washed twice in cold PBS buffer (10-folds volume of tissue mass) with protease inhibitor cocktail (Roche, Switzerland). The washed tissue pieces were transferred into HEPES buffer (5-folds volume of tissue mass, 0.25 mM sucrose, 25 mM HEPES at pH 7.4, 50 mM NaF, 0.25 mM Na_3VO_4, 0.25 mM PMSF, 2.5 mM EDTA, and 1mg/mL protease inhibitor cocktail). The tissue samples were homogenized 5-6 times using a Polytron electric homogenizer (Model PRO200, PRO Scientific Inc., Oxford, CT, USA) for 5-7 s on ice. The homogenate was centrifuged at 120,000 g for 30 min at 4 °C, and the supernatant was removed to deplete most of blood contamination. The remaining pellet was extracted with HEPES buffer (3 folds volume of tissue mass) and then centrifuged at 16,000 g at 4 °C for 30 min. The protein concentration of each sample was determined using the Bradford assay (Bio-Rad, Hercules, CA) in accordance with the manufacturer's protocol. Each protein sample (10 µg) was reduced with 20 mM dithiothreitol at 65 °C and alkylated with 25 mM iodoacetamide at room temperature, with each step requiring 1 h. The samples were all adjusted to a pH of 8. Modified trypsin (1:50 (w/w) (trypsin/protein) was added to each sample, which were then incubated overnight at 37 °C for 20 h to allow for complete digestion. The 5% of acetonitrile with 1% formic acid was added into each sample to stop the reaction. The

samples were centrifuged at 16,000 g at 4 °C for 1 h before the supernatants were obtained for further mass spectrometry analyses.

Mass spectrometry analyses A Q Exactive mass spectrometer (Thermo Scientific, Bremen, Germany) with a nanoelectrospray ion source (ThermoElectron, San Jose, CA) coupled to a nano flow UPLC (Waters LC nanoACQUITY, MA, USA) were used to perform MS analyses. A 180 µm × 20 mm trap column (Symmetry C18) and a 75 µm × 100 mm Waters C18 analytical column (1.7 µm particle BEH) with mobile phases A (0.1 % formic acid in water) and B (0.1 % formic acid in acetonitrile) were also used. The pump flow rate was set to 0.35 µL/min, and peptides (1 µg) were contained in the trap column for 10 min before elution was achieved. In doing so, a linear gradient of 5-35% B was used for the first 130 min followed by a rapid increase to 95% B over the following 20 min, while the column temperature was kept at 28 °C. The electrospray voltage was set at 1.9 kV. The Orbitrap mass analyzer performed full MS scans over the range m/z 300–2000 with a mass resolution of 70,000 (at m/z 200). The automatic gain control (AGC) target value was 1.00E+06 with a maximum injection time set at 100 ms. The 15 most intense ions with charge states ≥ 2 were fragmented in the HCD collision cell using a normalized collision energy of 30%. Tandem mass spectra were acquired in the Orbitrap mass analyzer set to a mass resolution of 17,500 at m/z 200 (AGC target 1.00E+05, 30 ms maximum injection time). The ion selection threshold was 3,300 for MS/MS. Dynamic exclusion of the sequenced peptides for 20 s was the method by which the repeat sequencing of peptides was minimized.

Protein identification and quantification The SEQUEST-based Proteome Discoverer (Thermo Scientific; version 1.4) was used to analyze all MS/MS samples. Considering the porcine database data only provides limited coverage, searches were performed using the human database (20,232 entries) combined with the porcine database (1,411 entries) from the Uniprot-Swissprot database (released January, 2013). The search settings that were used allowed for data containing two missed cleavages and the mass tolerances for the precursor and fragment ion mass were 10 ppm and 0.02 Da. The carbamidomethyl of cysteine was specified as a fixed modification, whereas deamidated asparagine and glutamine as well as oxidated methionine were set as variable modifications. The data was further searched against a decoy database and filtered using a 1% false discover rate (FDR). Peptides with high confidence, rank 1, and delta Cn < 0.1 were accepted. The function that included distinct proteins in the search was enabled. The Proteome Discoverer plugin, InforSense, was used for collecting gene ontology (GO) data. Further information regarding other relevant biological processes for each protein was retrieved from the AmiGo database. For quantification, the area under the curve of each peptide was calculated using Proteome Discoverer and the average of the three most abundant distinct peptides. This value represented the protein intensity. All of the given protein intensities were presented in Log10 form. After transformation, the intensity of each protein in the sample was divided by the sum of total proteins within the sample for normalization. The minimum protein intensity in each run divided by 3 gave the undetectable protein intensity.

Bioinformatics and statistical analyses The MultiExperiment Viewer (MeV v4.9) was used to perform the hierarchical cluster and heat map analyses (HCA), and the proteins were then clustered according to their Pearson correlation coefficients. STRING database was used to enrich certain subcellular locations and biological processes. Any

gene ontology (GO) biological processes and networks with a false-discovery rate (FDR) < 0.01 were considered to be significant in the analyses. A statistically significant p value less than 0.05 was required for the two-tailed tests. All the results are shown as the mean ± S.E. The nonparametric Mann-Whitney U test and ANOVA were employed to analyze the all differences between groups.

Differentiation of hiPSCs into CMs

The hiPSCs used in this investigation were from two lines that had been reprogrammed from human dermal fibroblasts and maintained in hiPSC growth medium as described (Ye et al., 2013). Karyotype analyses confirmed that the cells' chromosomal structure was normal (Figure S1).

hiPSCs were differentiated into CMs via a monolayer method. Isolated areas of contracting cells typically appeared on Day 7 after initiation of the CM differentiation protocol. Large contracting cluster was observed at Day 5 (Movie S1) and Day 130 (Movie S2). Flow cytometric analyses for cTnT expression suggested that the overall efficiency of the protocol was 68±15% and could reach as high as 83%. The hiPSC-CMs were obtained from the differentiation culture via micro-dissection on day 7 or 8 after contractions were observed and then enriched by preplating. Large clusters of contracting cells were collected, enzyme-treated, and preplated for at least 3 hours, which allowed the non-cardiomyocyte cells to adhere to the surface of the culture dish. The cell suspension, which contained individual hiPSC-CMs or small clusters of hiPSC-CMs, was collected and cultured on a Matrigel-coated surface (Movie S3). The cells became enlarged and flattened in 2 weeks.

Functional beneficial effects of cellular therapies are associated with differential protein expressions in recipient myocardium as revealed by global quantitative proteomics*.*

The mechanisms underlying the beneficial effects of stem cell treatment in myocardial regeneration are not well defined. The direct contribution of myocytes derived from the engrafted cells to the improved LV ejection fraction appears to be only part of the mechanism as the engraftment rate is low a few weeks after the cell transplantation. Because of the LV chamber function is improved a few weeks after the cell therapy the improved LV contractile performance is likely related to the changes of the recipient myocardium deferential expression profile of proteins (which could be the consequences of reduction of LV wall stress). We have reported that the LV functional beneficial effects of cell therapy results in reduction of LV wall stress (Xiong et al., 2013), which is accompanied by promoting endogenous cardiac progenitor cells (CPC) to injury site to repair.

Here we have taken a global proteomic approach to examine the infarct boarder zone myocardial changes in protein expression profiles after cell therapy using the hiPSC derived vascular cells (hiPSC-VC) (Xiong et al., 2013), which includes the ECs and SMCs. Specifically, we analyzed the expression profiles on myocardial tissue of pigs from 3 different groups: SHAM (n=5), LAD ligation (MI, N=5), and MI+ hiPSC-VC (n=5). A total of 1077 proteins were detected for SHAM and 1096 for MI groups versus 1000 proteins identified for MI+hiPSC-VCs (Figure S6A). A significant overlap of the

identified proteins in different groups was observed which underscores the high reproducibility of this label-free quantitative proteomics method.

We have confidently identified 66 proteins that were altered in the myocardium of MI hearts, but fully or partially recovered with cell transplantation. The top 20 enrichment results of the cellular component showed that the proteins were significantly localized in the extracellular region, membrane, mitochondrion, and cytoskeleton (Figure S6B). All of the altered proteins showed in the heatmap are found to be related to three major groups: regulation of metabolic processes, cytoskeleton organization, and regulation of energy processes (Figure S6C). The representative up- and down-regulated protein expression cases are summarized in Figure 6. The protein expression profiles changes substantially towards normalcy (Figure 6), which may be attributed to the improvement in wall stress associated with cell therapy (Figure 3).

Supplemental Figures

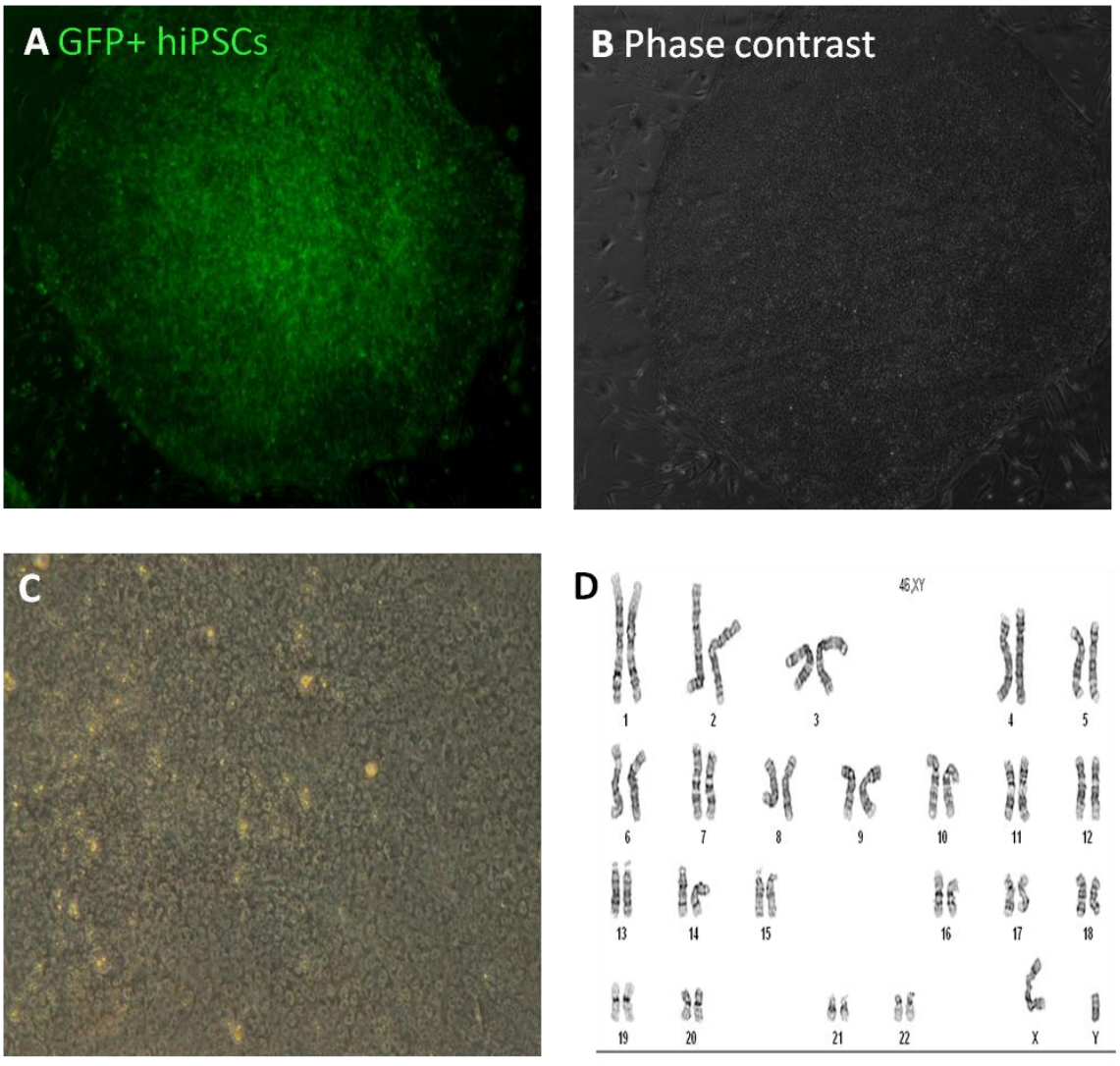

Figure S1: Characteristics of undifferentiated hiPSCs. The hiPSCs used for this investigation were from two lines that had been reprogrammed from human dermal fibroblasts and **(A)** were engineered to express GFP. When cultured as a monolayer with irradiated MEF, **(B)** the cells grew to form flat, compact colonies with distinct cell borders (phase contrast; magnification: 40x) and **(C)** displayed prominent nuclei and a high nucleus-to-cytoplasm ratio (light microscopy; magnification: 100x). **(D)** Karyotype analyses confirmed that the cells' chromosomal structure was normal. (Related to Figure 1)

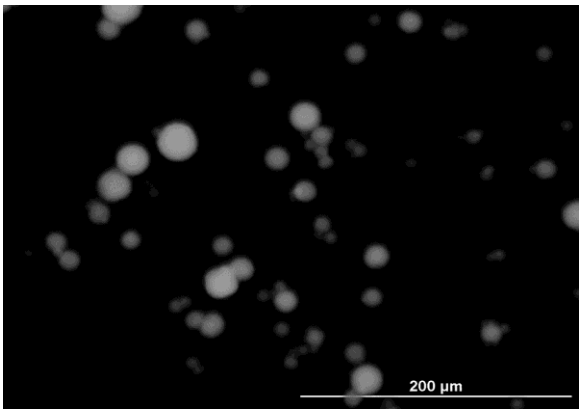

Figure S2 Extended IGF-1 administration. The duration of IGF-1 administration was extended by encapsulating the protein in gelatin microspheres, which were added to a fibrin patch created over the site of myocardial injury. Bar=200 µm. (Related to Figure 3)

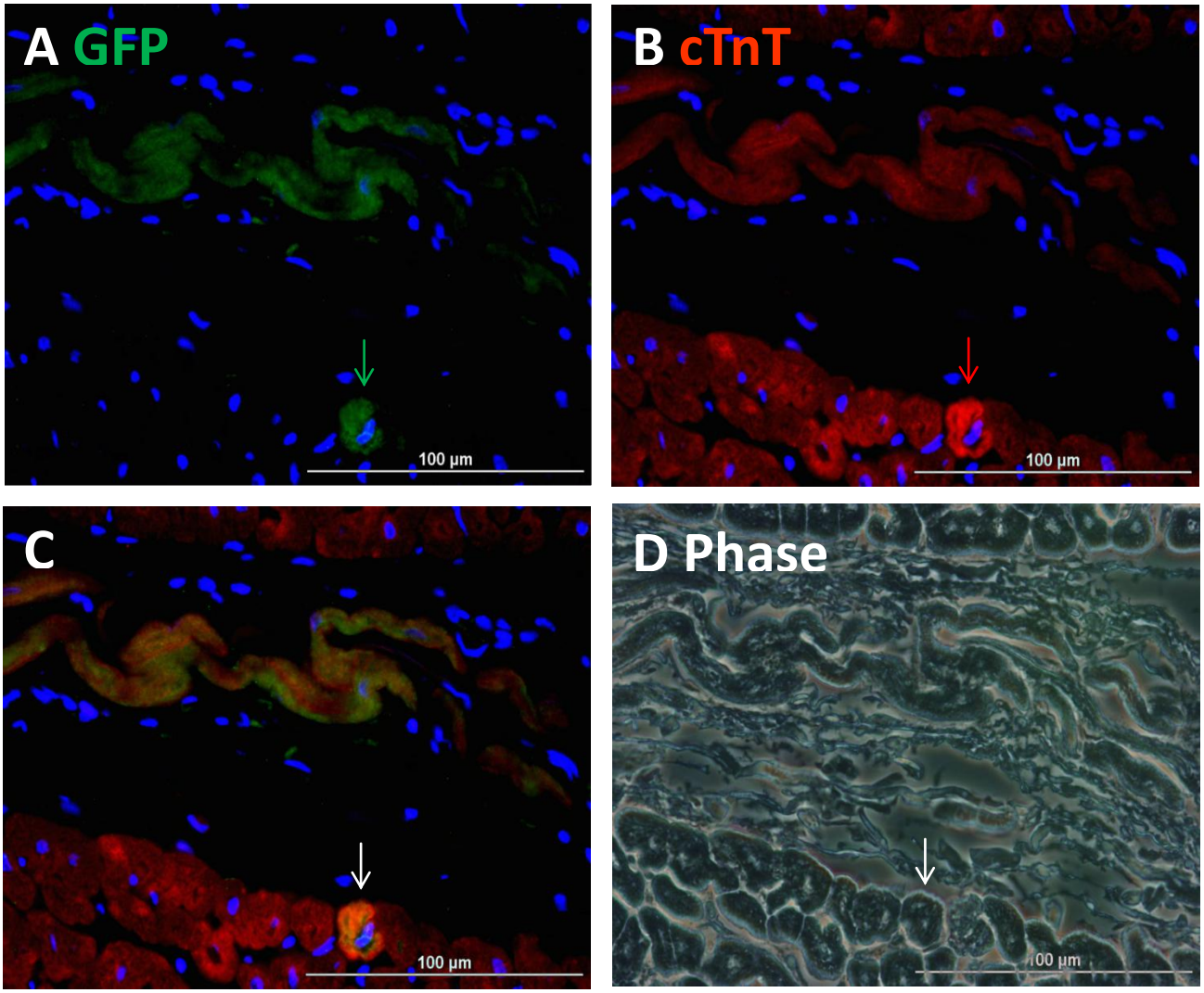

Figure S3. Transplanted hiPSC-CMs were rarely observed in native muscle fibers. Engraftment of the injected cells was evaluated in sections stained for the presence of **(A, C)** GFP; muscle fibers were visualized via **(B, C)** fluorescent immunostaining for cTnT, and nuclei were counterstained with DAPI. **(D)** The sections displayed in A-C were imaged with a phase-contrast microscope. The arrow identifies a muscle fiber that contains a transplanted cell. Bar=100 µm. (Related to Figure 2)

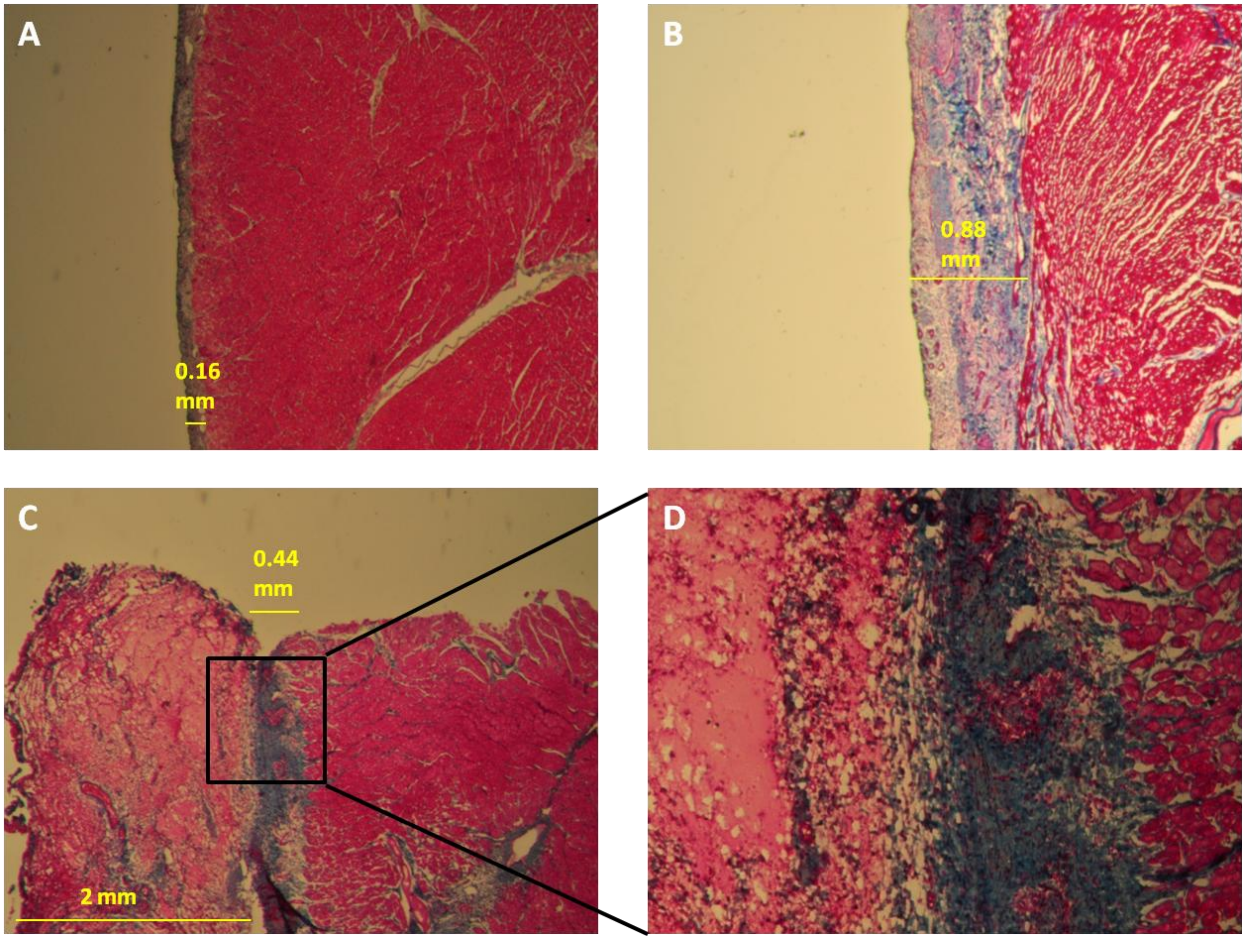

Figure S4. Patch transplantation increases wall thickness. Masson-trichrome–stained sections from the hearts of animals in the (**A**) Sham and (**B**) MI groups and from (**C-D**) the hearts of animals treated with the IGF-1–containing patch were examined for evidence of patch integration (Magnification: A-C=25x; D=100x). (Related to Figure 3)

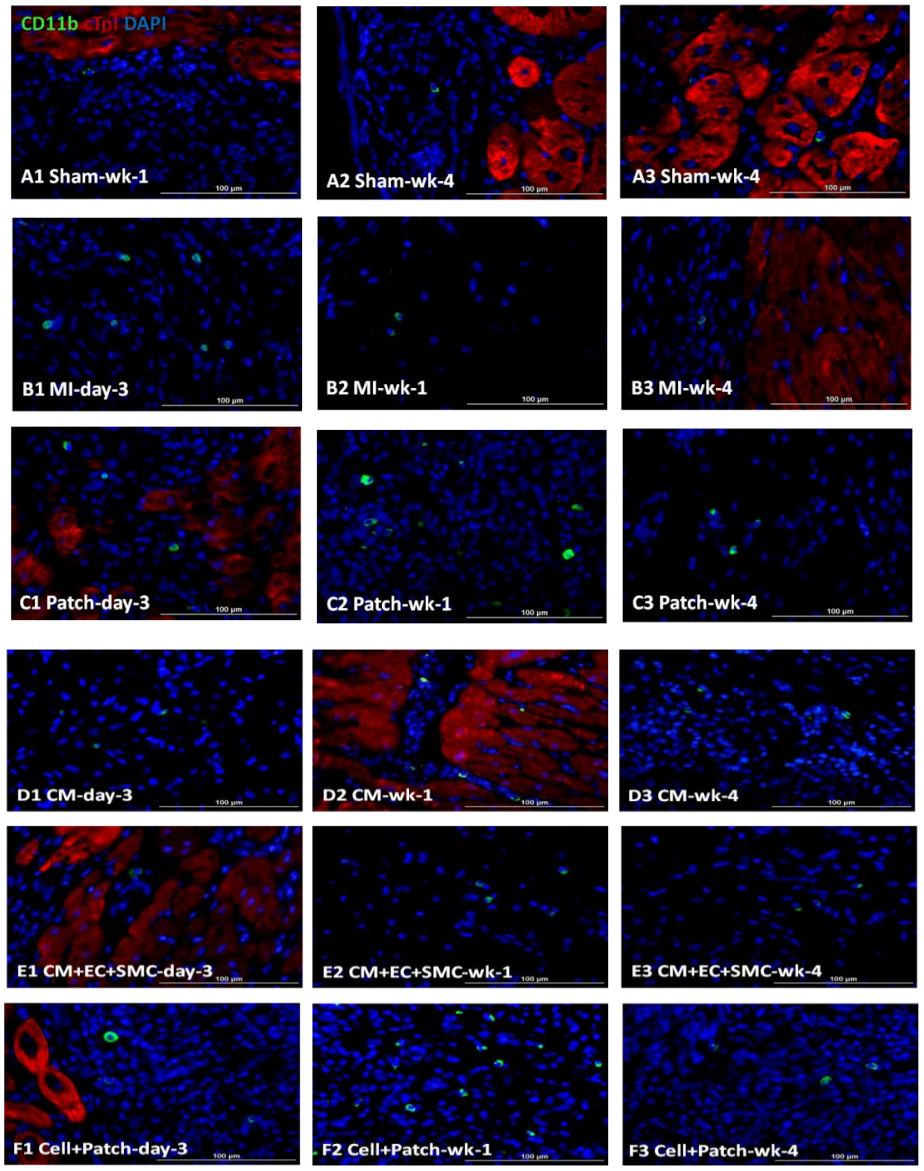
CD11b cTnI DAPI
A1 Sham-wk-1
A2 Sham-wk-4
A3 Sham-wk-4
B1 MI-day-3
B2 MI-wk-1
B3 MI-wk-4
C1 Patch-day-3
C2 Patch-wk-1
C3 Patch-wk-4
D1 CM-day-3
D2 CM-wk-1
D3 CM-wk-4
E1 CM+EC+SMC-day-3
E2 CM+EC+SMC-wk-1
E3 CM+EC+SMC-wk-4
F1 Cell+Patch-day-3
F2 Cell+Patch-wk-1
F3 Cell+Patch-wk-4

G

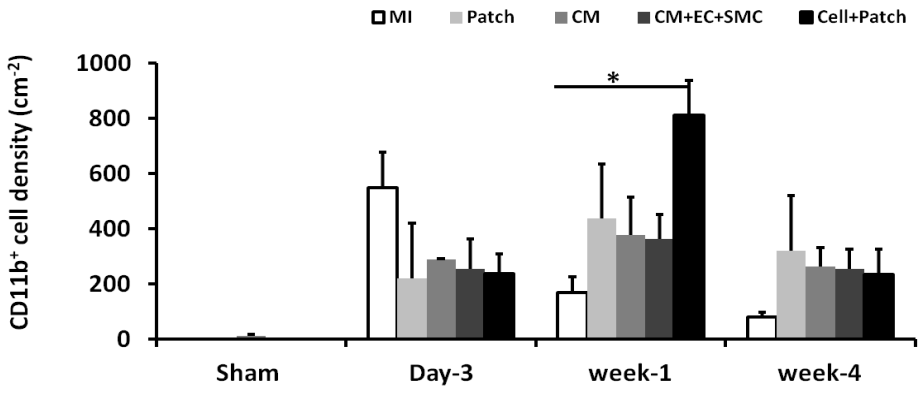
MI
Patch
CM
CM+EC+SMC
Cell+Patch
CD11b+ cell density (cm-2)
1000
800
600
400
200
0
*
Sham
Day-3
week-1
week-4

Figure S5: Inflammation was delayed and moderately increased in animals treated with both hiPSC-derived cardiac cells and the IGF-1–containing patch. Sections from the infarct zone and the border zone of the infarct in hearts from **(A1-A3)** Sham **(B1-B3)** MI, **(C1-C3)** Patch, **(D1-D3)** CM, **(E1-E3)** CM+EC+SMC, and **(F1-F3)** Cell+Patch hearts were obtained at Day 3, Week 1, and Week 4 after injury. Immunofluorescently stained for expression of the inflammatory-cell marker CD11b; cardiac muscle fibers were visualized via immunofluorescent staining for cTnI and nuclei were counterstained with DAPI. **(G)** Inflammation was evaluated by quantifying the density of $CD11b^+$ cells at each time point. *$p<0.05$; bar=100 μm. (Related to Figure 5)

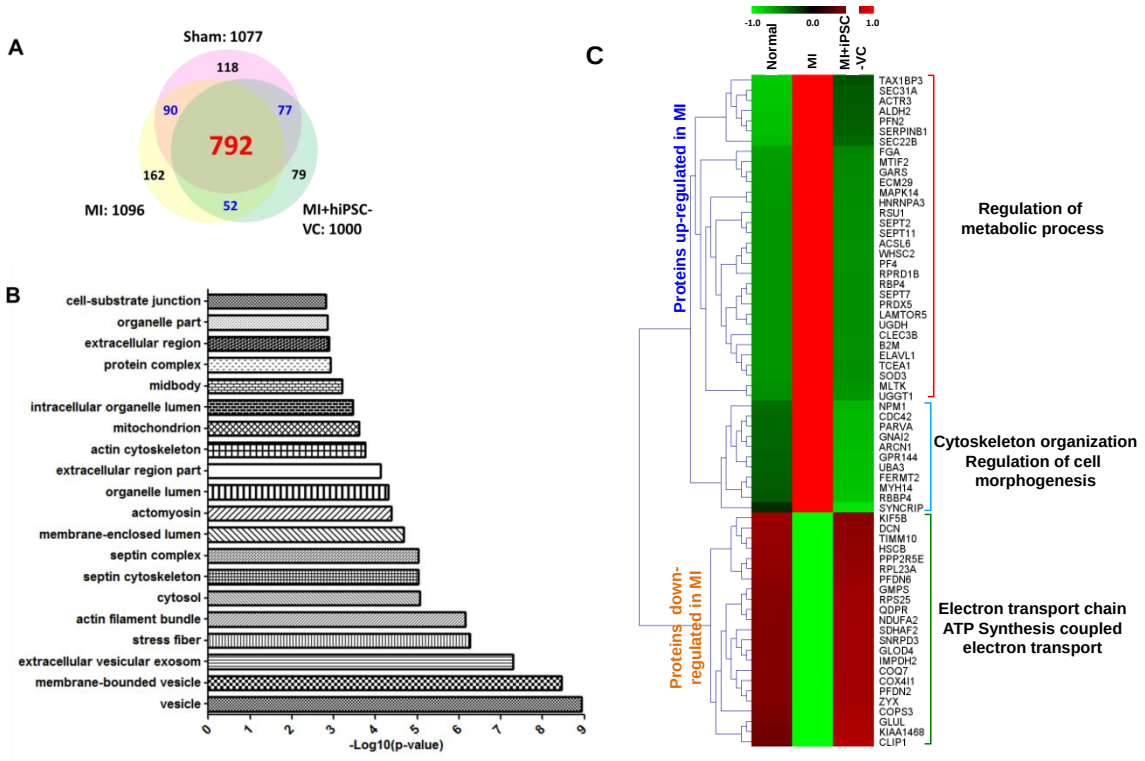

Figure S6. ***Myocardial protein expression profiles.*** Myocardial protein expression profiles were evaluated in animals that had been treated with (MI+hiPSC-VCs) or without (MI) hiPSC-VC transplantation after experimentally induced MI; control assessments were performed in animals that underwent all surgical procedures for the induction of MI except for the ligation step (Sham). **(A)** The number and distribution of proteins detected in each of the three treatment groups is illustrated with a Venn diagram. **(B)** The cellular (or extracellular) locations of 66 proteins whose expression levels were altered in MI hearts and fully or partially restored in MI+hiPSC-VC hearts was evaluated with STRING software; the 20 most significant locations are shown. (**C).** The functional categories for 66 proteins whose expression levels were altered in MI hearts and fully or partially restored in MI+hiPSC-VC hearts were evaluated and displayed as a heat map. Hierarchical clusters and heat map analyses were performed with MultiExperiment Viewer software (MeV v4.9); proteins were clustered according to their Pearson correlation coefficients, and STRING software was used to enrich certain biological processes. The proteins up-regulated by MI were involved in the regulation of metabolic processes, cytoskeletal organization, and morphogeensis. The proteins down-regulated in MI may regulate processes. (Related to Figure 6)

Table S1. Sample size of animal groups

	Day-3	Week-1	Week-4
Sham group	0	3(3)	9(6)
MI group	4(4)	4(4)	11(7)
Patch group	3(3)	3(3)	8(7)
CM group	3(3)	4(4)	6(3)
CM+EC+SMC group	3(3)	3(3)	6(3)
Cell+Patch group	4(4)	3(3)	12(8)
ECG monitoring/electro-physiology studies			
MI group			6
Patch group			2
Patch+CM group			8
Total	**17(17)**	**20(20)**	**68(34)**

The numbers in the bracket are the animal number used for evaluation of immunohistochemistry. MI= Myocardial infarction; CM= Cardiomyocyte; EC= Endothelial cell; SMC= Smooth muscle cell Cell= CM+EC+SMC; ECG= Electrocardiogram.

(Related to Figure 3)

Table S2. Cytokine releasing profile of hiPSC differentiated cells

		hiPSC-ECs	hiPSC-SMCs	hiPSC-CMs
Growth factor, cytokine	**Angiogenin**	55420±6688	14336±915	52468±4118.9
	Angiopoietin-1	1219±172	7774±230	3770±313.5
	Angiopoietin-2	11654±6097	764±120	1006±146.3
	IL-6	44737±17630	2137±269	5079±391.5
	PDGF-BB	2041±250	295±50	24±5.9
	VEGF	24±0	17±0	477±188
	TGF-beta1	624±40	728±22	659±32.4
Chemokine	**Growth regulated protein**	55015±3591	3372±110	7942±785.1
	IL-8	22573±3578	2793±52	4262±1261
	MCP-1	62393±24	62895±1975	61048±713.5
	MCP-3	1152±204	508±28	16139±2773
	RANTES	1467±272	1448±54	90±0.5
Inhibitor of metalloproteinases	**TIMP-1**	12930±7029	17693±6309	12478±4154.7
	TIMP-2	7049±2199	11868±2028	7984±1685.8
Angiogeic inhibitor	**Angiostatin**	210±37	236±25	254±25.7
	Endostatin	550±77	154±63	296±4.1
Proteases	**MMP-9**	702±288	190±3	155±2.2
Plasminogen activator	**uPAR**	3102±57	2533±315	1048±64.6
Angiogeic receptor	**VEGFR2**	672±16	145±21	176±0.4
	VEGFR3	287±15	316±16	285±34.5
	Tie-2	171±28	210±47	218±10.1

hiPSC= Human induced pluripotent stem cells; EC= Endothelial cell; SMC= Smooth muscle cell; CM= Cardiomyocyte; IL-6= Interleukin-6; PDGF-BB= Platelet-derived growth factor; VEGF= Vascular endothelial growth factor; TGF-beta1= Transforming growth factor- beta1 IL-8= Interleukin-8; MCP-1= Monocyte chemoattractant protein-1; MCP-3= Monocyte chemoattractant protein-3; RANTES = Regulated upon activation normal T cell expressed and presumably secreted; TIMP-1= tissue inhibitors of metalloproteinases-1; TIMP-2= tissue inhibitors of metalloproteinases-2; MMP-9= Matrix metallopeptidase 9; uPAR= Urokinase receptor; VEGFR2 = Vascular endothelial cell growth factor receptor2; VEGFR3 = Vascular endothelial cell growth factor receptor3.
(Related to Figure 2)

Movie Legends

Movie S1: A sheet of contracting hiPSC-CMs at 5 days after contractions were first observed. (Related to Figure 1).
Movie S2: Contraction of a sheet of hiPSC-CMs at 130 days after contractions were first observed. (Related to Figure 1).
Movie S3: hiPSC-CMs after 6 days of culture on a Matrigel-coated surface: monolayer of contracting hiPSC-CMs (magnification:200x). (Related to Figure 1).

REFERENCES

Feygin, J., Mansoor, A., Eckman, P., Swingen, C., and Zhang, J. (2007). Functional and bioenergetic modulations in the infarct border zone following autologous mesenchymal stem cell transplantation. American journal of physiology Heart and circulatory physiology *293*, H1772-1780.

Jerosch-Herold, M., Swingen, C., and Seethamraju, R.T. (2002). Myocardial blood flow quantification with MRI by model-independent deconvolution. Med Phys *29*, 886-897.

Xiong, Q., Du, F., Zhu, X., Zhang, P., Suntharalingam, P., Ippolito, J., Kamdar, F.D., Chen, W., and Zhang, J. (2011a). ATP production rate via creatine kinase or ATP synthase in vivo: a novel superfast magnetization saturation transfer method. Circulation research *108*, 653-663.

Xiong, Q., Hill, K.L., Li, Q., Suntharalingam, P., Mansoor, A., Wang, X., Jameel, M.N., Zhang, P., Swingen, C., Kaufman, D.S.*, et al.* (2011b). A Fibrin Patch-Based Enhanced Delivery of Human Embryonic Stem Cell-Derived Vascular Cell Transplantation in a Porcine Model of Postinfarction LV Remodeling. Stem Cells *29*, 367-375.

Xiong, Q., Ye, L., Zhang, P., Lepley, M., Swingen, C., Zhang, L., Kaufman, D.S., and Zhang, J. (2012). Bioenergetic and functional consequences of cellular therapy: activation of endogenous cardiovascular progenitor cells. Circulation research *111*, 455-468.

Xiong, Q., Ye, L., Zhang, P., Lepley, M., Tian, J., Li, J., Zhang, L., Swingen, C., Vaughan, J.T., Kaufman, D.S.*, et al.* (2013). Functional consequences of human induced pluripotent stem cell therapy: myocardial ATP turnover rate in the in vivo swine heart with postinfarction remodeling. Circulation *127*, 997-1008.

Ye, L., Haider, H., Tan, R., Toh, W., Law, P.K., Tan, W., Su, L., Zhang, W., Ge, R., Zhang, Y.*, et al.* (2007). Transplantation of nanoparticle transfected skeletal myoblasts overexpressing vascular endothelial growth factor-165 for cardiac repair. Circulation *116*, I113-120.

Ye, L., Zhang, S., Greder, L., Dutton, J., Keirstead, S.A., Lepley, M., Zhang, L., Kaufman, D., and Zhang, J. (2013). Effective cardiac myocyte differentiation of human induced pluripotent stem cells requires VEGF. PloS one *8*, e53764.

Zeng, L., Hu, Q., Wang, X., Mansoor, A., Lee, J., Feygin, J., Zhang, G., Suntharalingam, P., Boozer, S., Mhashilkar, A.*, et al.* (2007). Bioenergetic and functional consequences of bone marrow-derived multipotent progenitor cell transplantation in hearts with postinfarction left ventricular remodeling. Circulation *115*, 1866-1875.

Zhang, J., Klos, M., Wilson, G.F., Herman, A.M., Lian, X., Raval, K.K., Barron, M.R., Hou, L., Soerens, A.G., Yu, J.*, et al.* (2012). Extracellular matrix promotes highly efficient cardiac differentiation of human pluripotent stem cells: the matrix sandwich method. Circulation research *111*, 1125-1136.